PDG/REM/RDT/LCSM, IFREMER
Benoît GAURIER • Grégory PAYNE • Thomas BACCHETTI • Jean-Valéry FACQ • Grégory GERMAIN • Gohar SHOUKAT
Date : 17.06.2021

FORCE VARIATIONS MEASUREMENT ON A TIDAL TURBINE MODEL DUE TO TOWER PROXIMITY

Experiment summary

Fiche documentaire

Titre du rapport : Force variations measurement on a tidal turbine model due to tower proximity - Experiment summary	
Référence interne : 08CSMBL21 **Diffusion :** □ libre (internet) ☑ restreinte (internet) - date de levée d'embargo : □ interdite (confidentielle) - date de levée de confidentialité :	**Date de publication :** 17.06.2021 **Version :** 1.0.0 **Référence de l'illustration de couverture :** Crédit photo/titre/date **Langue(s) :** Français - Anglais
Résumé / Abstract : This document presents the experimental tests carried out in the wave and current flume tank of IFREMER at Boulogne-sur-mer, France. The main objective of these tests is to quantify the effects of the tower proximity on the force variations of a horizontal axis tidal turbine.	
Mots clés / Key words : horizontal axis tidal turbine, performance measurement, force variations, laser doppler velocity measurements, tower proximity	
Comment citer ce document :	
Disponibilité des données de recherche :	
DOI : https://doi.org/10.17882/81077	

Commanditaire du rapport :	
Nom / référence du contrat : ☐ Rapport intermédiaire ☑ Rapport définitif	
Projets dans lesquels ce rapport s'inscrit : R&D Hydroliennes P204-0033 - FP3357	
Auteur(s) / Adresse mail Benoît GAURIER / bgaurier@ifremer.fr Grégory PAYNE / gregory.payne@ec-nantes.fr Thomas BACCHETTI / tbacchet@ifremer.fr Jean-Valéry FACQ / jvfacq@ifremer.fr Grégory GERMAIN / ggermain@ifremer.fr Gohar SHOUKAT / gohar.shoukat@eleves.ec-nantes.fr	**Affiliation** PDG/REM/RDT/LCSM, IFREMER LHEEA - École Centrale de Nantes PDG/REM/RDT/LCSM, IFREMER PDG/REM/RDT/LCSM, IFREMER PDG/REM/RDT/LCSM, IFREMER LHEEA - École Centrale de Nantes
Encadrement(s) :	
Destinataire :	
Validé par :	

Contents

1 Experimental facility **5**

2 Instrumentation **6**

2.1 Laser Doppler Velocimeter 6

2.2 Hexapod 7

2.3 Marine Current Turbine Model 7

2.4 Acquisition system 9

3 Setup **9**

4 Acquisitions **11**

References **16**

Introduction

The purpose of the experiments is to quantify the effect of the tower proximity on the force variations of a horizontal axis tidal turbine model. The blade forces variations are especially difficult to understand and to simulate. Consequently, this is the same case for the rotor and finally for the complete turbine. Such variations have already been experimentally observed by Payne et al. (2018) and numerically studied by Mason-Jones et al. (2013). Their origins are however not completely understood and explained (Deskos et al. 2020). They have never been specifically studied for now.

Several reasons can explain such blade forces variations at the rotation frequency. The tower proximity, first, generating a velocity modification downstream to the rotor. In that case, an unexpected phase lag has been observed by Payne et al. (2018) between the vertical position of the tower and the angles of the maximum and minimum of the forces. The flow turbulence rate associated with a velocity shear profile can be another source of blade forces variations as shown by Gaurier et al. (2020a). The contribution to the blade forces variations of the turbulent velocity shear profile comparing to the tower shadowing effects has never been studied for now.

1 Experimental facility

The tests take place in the wave and current flume tank of IFREMER at Boulogne-sur-mer, France. The experimental working section is 4 m wide by 2 m deep and 18 m length (figure 1). Two pumps generate a turbulent flow with a speed range between 0.1 to 2.2 m/s.

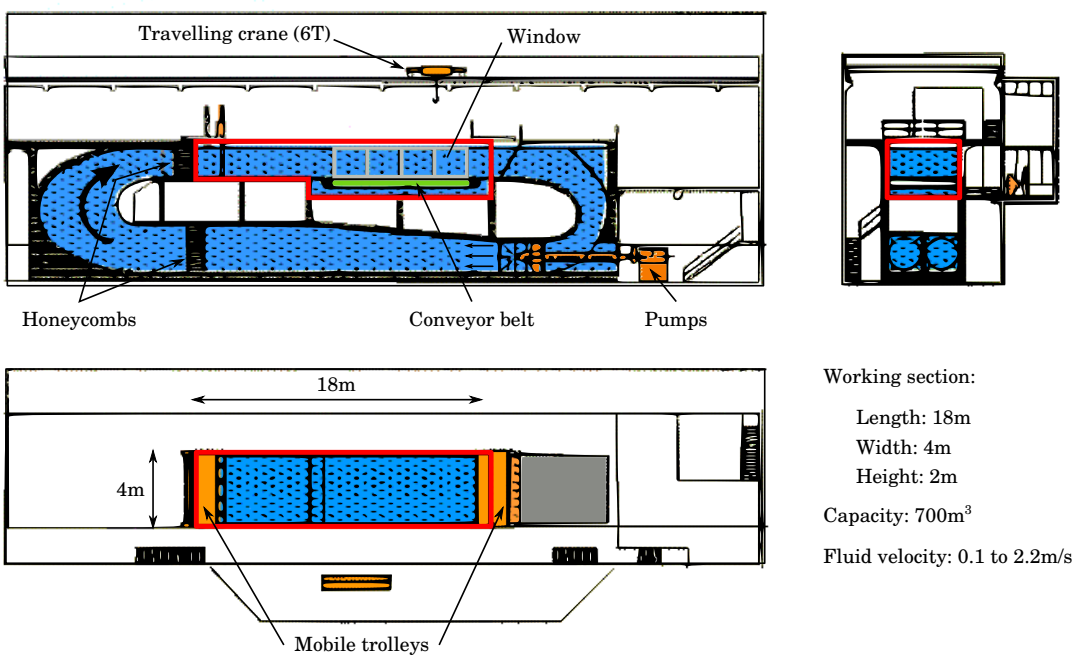

Figure 1 – Schematic of the wave and current flume tank

The turbulent intensity rate can be regulated by the use of flow straightener and grid. With both of them, the turbulent intensity is about $I_\infty \simeq 1.5\,\%$. When the grid and the flow straightener are removed, I_∞ reaches values of about 15 %. These turbulent values are constant along the test area, because it is self-sustaining by the two pumps generating the flow in the tank.

More informations about the flume tank can be found in Gaurier et al. (2018).

2 Instrumentation

2.1 Laser Doppler Velocimeter

This technique enables the measurement of the velocity to be carried out, at a single point in a flow field, with a high temporal resolution. The 3-components LDV system (see figure 2) includes 6 laser beams with 3 different wave lengths: 514 nm, 488 nm and 532 nm.

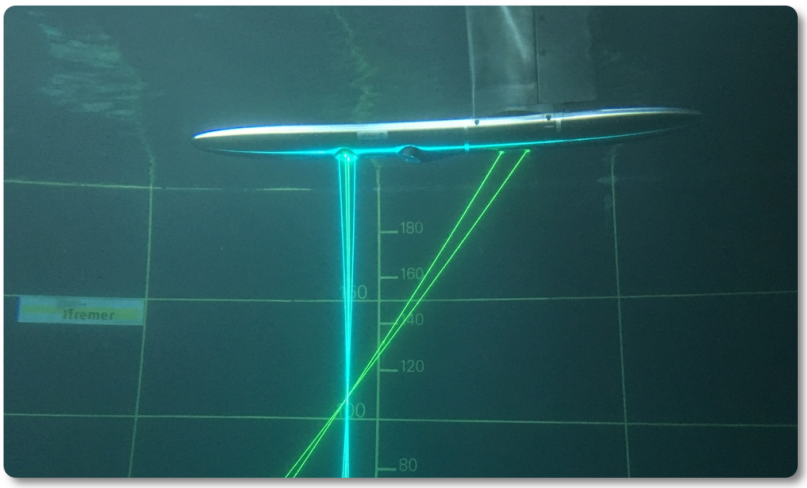

Figure 2 – The 3 components Laser Doppler Velocimeter probe used in the IFREMER flume tank

Whenever a reflecting particle entrained in the fluid passes through the intersection of two laser beams, the scattered light received from the particle fluctuates in intensity. LDV makes use of the fact that the frequency of this fluctuation is equivalent to the Doppler shift between the incident and scattered light, and is thus proportional to the component of the particle velocity (Dantec Dynamics 2018). The water of the tank is seeded with particles which should be small enough to follow the flow, yet large enough to scatter sufficient light to obtain a good signal-to-noise ratio. Typically the size of particles used in the IFREMER flume tank is 10 μm. These particles are spherical and composed of silver coated glass. The data-rate depends on the number of particles detected by the system. The sampling frequency is consequently irregular due to the fact that one measurement value corresponds to one detected particle in the volume.

The 3-components LDV measurement is not direct because of the probe shape and arrangement. Considering the velocity vector $\overrightarrow{U} = u \cdot \vec{e_x} + v \cdot \vec{e_y} + w \cdot \vec{e_z}$, the three components are projected according to the equation 1, with LDAi corresponding to the beam measurements.

$$\begin{pmatrix} u \\ v \\ w \end{pmatrix} = \begin{pmatrix} 0.005247 & 1.004515 & -0.005563 \\ 0.999819 & -0.013590 & 0.008014 \\ 0.038989 & 1.412896 & -1.734007 \end{pmatrix} \cdot \begin{pmatrix} \text{LDA1} \\ \text{LDA2} \\ \text{LDA3} \end{pmatrix} \tag{1}$$

Because the 3-components LDV system is used in non-coincident mode, note that before applying such matrix operation, the LDAi measurements need to be interpolated using the same timestamp.

The 3-components LDV probe is fixed on a traverse system used to automatically move the measurement point. This traverse system has its own axis orientation, which is different from the one used for the 3C-LDV. To compare these different axis systems better, schematic 3 depicts both the 3C-LDV system, the traverse system and their corresponding axis orientations in the tank.

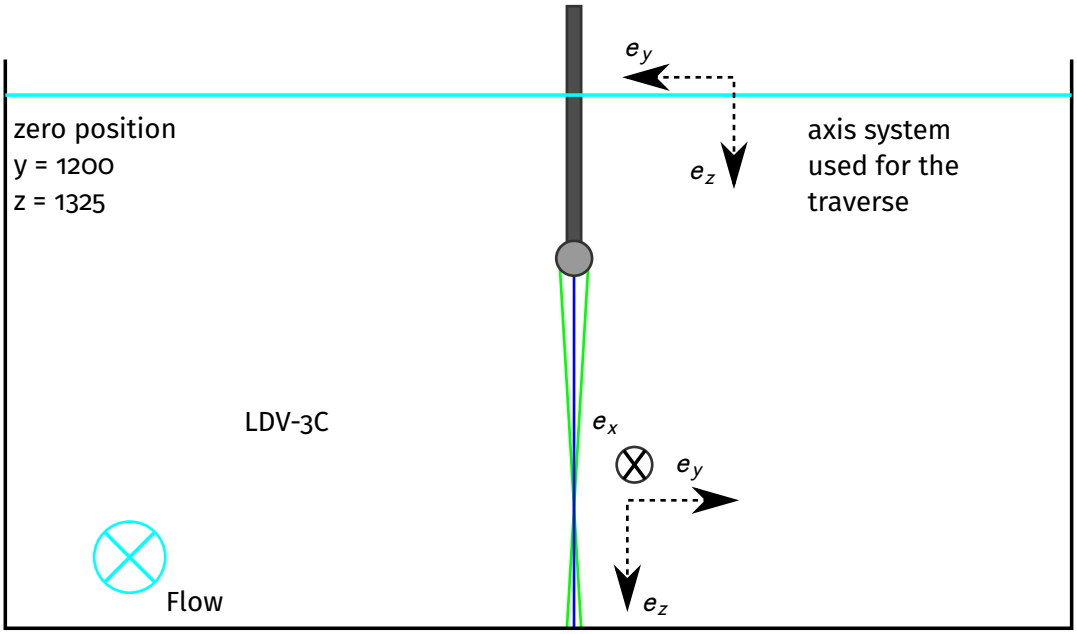

Figure 3 – Schematic of the different axis for both the 3C-LDV system and for the traverse system. The zero position corresponds to the y and z coordinates when the 3C-LDV is at the very centre of the tank (same position as the turbine hub).

Table 1 – Highest characteristics of the dynamic motion created by the hexapod

motion	amplitude	velocity	acceleration
Tx	±460 mm	±1 m/s	±10 m/s^2
Ty	±460 mm	±1 m/s	±10 m/s^2
Tz	±460 mm	±0.65 m/s	±8 m/s^2
Rx	±30°	±50 °/s	±500 °/s^2
Ry	±30°	±50 °/s	±500 °/s^2
Rz	±40°	±70 °/s	±700 °/s^2

2.2 Hexapod

The hexapod can be used for dynamic motion or precision positioning, following the six degrees of freedom: three translations and three rotations. Its load capability is 1 T with the motion characteristics given on table 1. In the laboratory, the hexapod is fixed on the crane and can be located above the free surface of the tank to support an experimental model into the water. The accuracy of the precision positioning is 0.5 mm according to the manufacturer Symétrie technology (2020).

2.3 Marine Current Turbine Model

A three-bladed horizontal axis turbine of $D = 0.724$ m in diameter is used during this testing campaign (figure 4). The blades length is 307 mm and the hub diameter is 110 mm. The distance between the blade axis and the tower axis is 594 mm, corresponding to 0.8 D.

The three blades are constituted of carbon fibres for a stronger stiffness. They all come from the same single moult to prevent shape differences. The blades are designed based on NACA 63-418 aerofoil and are of a similar geometry as those reported in previous studies (Gaurier et al. 2015; Gaurier et al. 2020b; Deskos et al. 2020).

The turbine rotor is connected to a motor-gearbox assembly consisting of a gearbox (1/26 ratio), a DC motor, a dump load and a motor speed control unit, providing an active rotor speed control, as described in Gaurier et al. (2017). For every test carried out in this dataset, the turbine works under a speed control strategy. The motor is also equipped with an encoder to measure the rotational speed of the rotor.

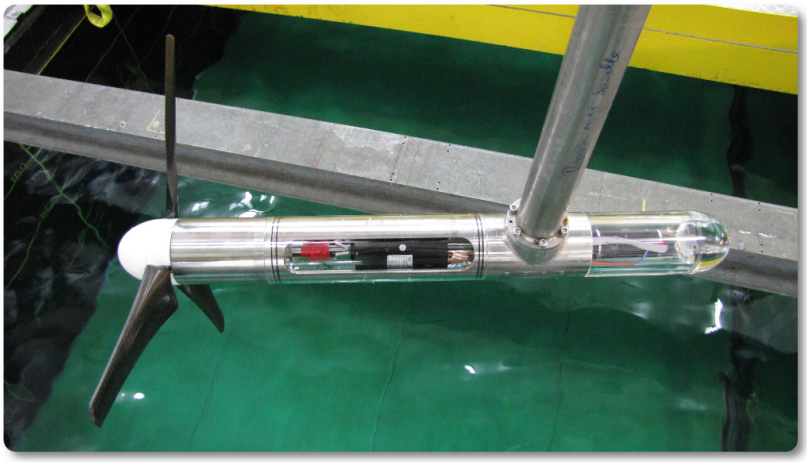

Figure 4 – View of the turbine model in the IFREMER flume tank

A waterproof transducer is positioned upstream of the rotor seals to measure the torque Q and thrust T produced by the rotor and prevent inaccurate measurements related to friction losses (figure 5). Each blade root is equipped with an individual load cell enabling multi-axial loadings to be captured: 2 forces and 3 moments. The measured forces correspond to the blade load contribution to torque (e_{xi}) and thrust (e_{yi}), respectively. The in and out of plane bending moments around each of the blades were captured by measuring the edge-wise bending moment (e_{xi}), the flap-wise bending moment (e_{yi}) and the pitching moment (e_{zi}), with $i = 1-3$ corresponding to the blade coordinate system (see schematic 5). The initial position is set when blade 1 is at the top-dead centre (see schematic 6).

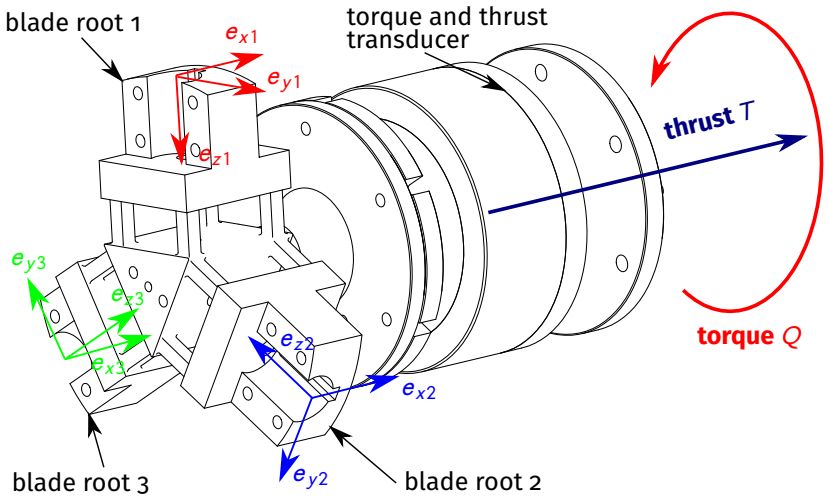

Figure 5 – The blade rood load cell with its three coordinate systems and the torque and thrust transducer

From these measured turbine parameters, it is then possible to calculate the main classical normalized performance coefficients: the thrust and power coefficients (equation 2).

$$C_P = \frac{P}{\frac{1}{2}\rho S U_\infty^3} \quad \text{and} \quad C_T = \frac{T}{\frac{1}{2}\rho S U_\infty^2} \tag{2}$$

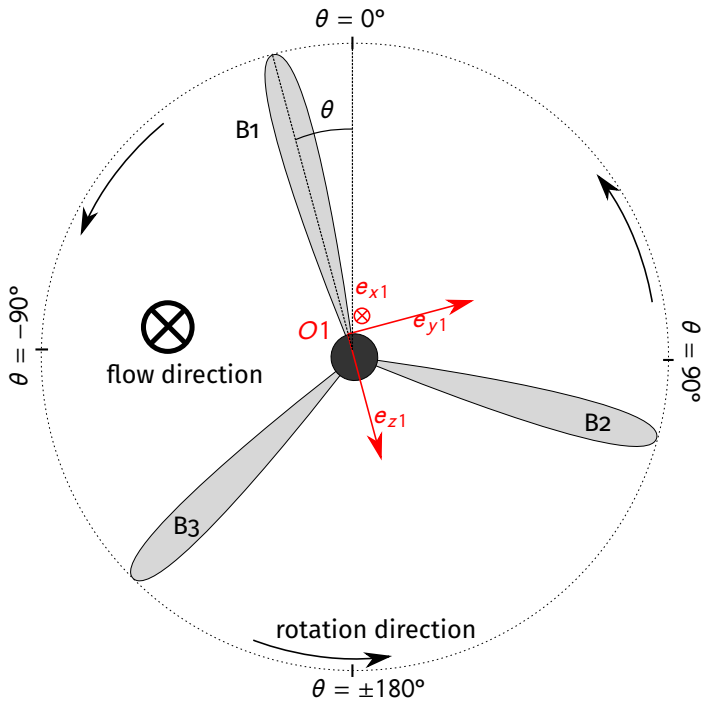

Figure 6 – Schematic of the turbine facing the flow, with the blade B1 root coordinate system. θ stands for the turbine angle of rotation, with $\theta = 0$ corresponding to blade B1 at top-dead centre. Note the sign convention for θ corresponding to the axis system orientation.

where P stands for the turbine power $P = \omega Q$, ρ is the water density and S is the rotor swept area with $S = \pi R^2$. Such parameters are classically plotted versus the normalized rotation speed of the turbine, i.e. the Tip Speed Ratio (TSR) which is defined as:

$$TSR = \frac{\omega R}{U_\infty} \tag{3}$$

with ω the turbine rotation speed expressed in rad/s.

2.4 Acquisition system

The shielded cables coming from the turbine transducers are routed through a slip ring, enabling continuous data transfer and power in or to the main acquisition system. These low voltage signals are amplified by an electronic signal processing unit, located on the upper section of the turbine assembly, avoiding water immersion of the electronics.

An in-house acquisition software, based on National Instrument Labview programming platform is used to record the turbine parameters. The acquisition hardware is based on modules PXIe-4339. These modules have a 24 bits resolution, with analogue input channels.

In addition, both the National Instruments platform and the 3C-LDV acquisition system are triggered using a 5 V digital signal. This ensures simultaneously start of the recording.

3 Setup

The experimental setup corresponds to the schematics presented on figure 7 with the turbine fixed underneath the hexapod and a dummy tower, represented in red on the schematic, located on the floor. This

schematic does however not exactly correspond to what has been realized during the tests: for practical reasons this is finally the turbine which has been fastened to the tank floor. The dummy tower was then fixed underneath the hexapod which varied the distance between the turbine rotor and this dummy tower, as depicted on figure 8, along the streamwise direction.

The 3C-LDV records the incoming velocity in synchronization with the turbine parameters. The velocity measurement point is located at 4 D upstream of the rotor in the streamwise direction and 20 cm above the rotation axis in the vertical spanwise direction.

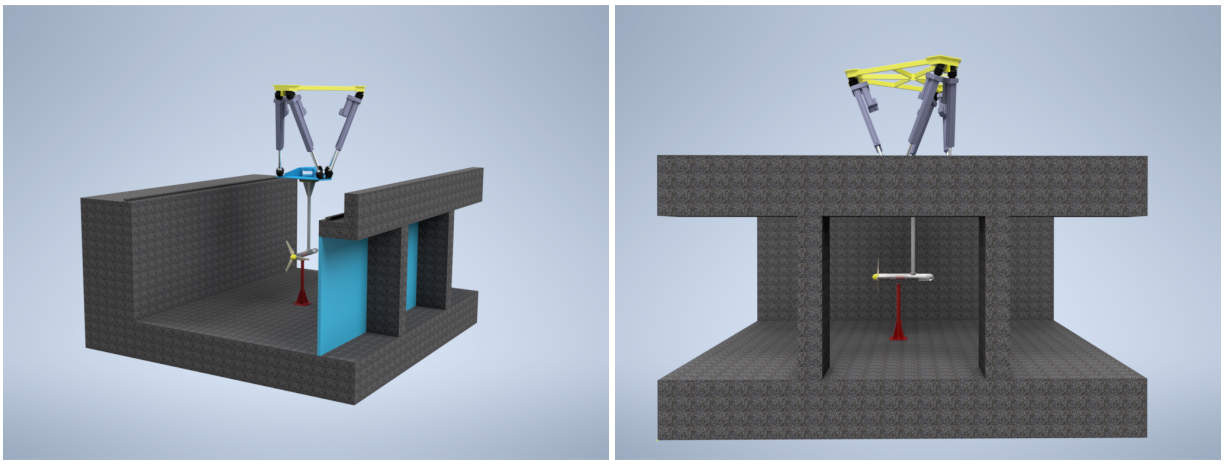

Figure 7 – Drawings of the initially planned setup with the hexapod supporting the turbine model and the dummy tower (in red) fixed on the tank floor. For practical reasons, this is the contrary which has finally been realized: the dummy tower was accurately positioned by the hexapod and the turbine model was fixed on the floor of the tank.

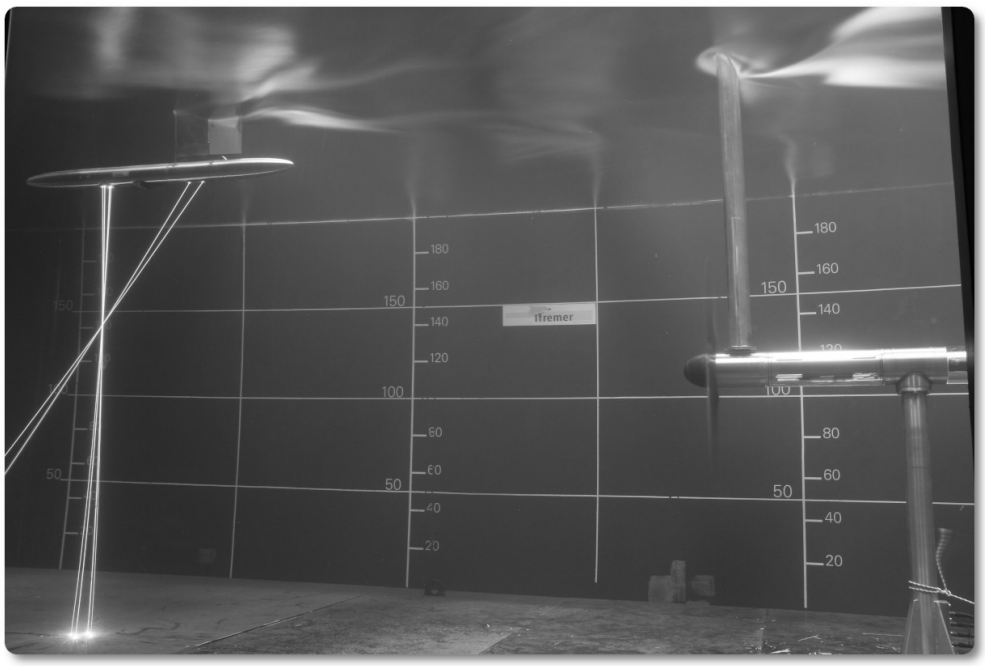

Figure 8 – Picture of the realized setup: the hexapod (not visible on this picture because above the free surface) supports the dummy tower above the turbine model which is fixed on the floor of the tank. On this picture, the dummy tower is located at the nearest possible position from the rotor. The 3C-LDV records the incoming velocity in synchronization with the turbine parameters. The velocity measurement point is located at 4 D upstream to the rotor in the streamwise direction and 20 cm above the rotation axis in the vertical spanwise direction.

Four distances between the dummy tower and the turbine rotor have been tested:

- position 0: this position corresponds to the exact same vertical position than the real turbine tower. The distance is 594 mm between the rotor axis and both the towers axis, i.e. 0.82 D.
- position 1: this position corresponds to a distance of 427 mm between the rotor and the dummy tower axis, i.e. 0.59 D.
- position 2: this position corresponds to a distance of 260 mm between the rotor and the dummy tower axis, i.e. 0.36 D.
- position 3: this position corresponds to a distance of 93 mm between the rotor and the dummy tower axis, i.e. 0.13 D.

For every distance, three flow velocities $U_\infty = 0.8$, 1.0 and 1.2 m/s and eleven turbine rotation speeds, between $TSR = 0$ and 7, have been selected[1]. The turbine performance has been quantified without the dummy tower as well, to generate a reference set of plots for all flow velocities and turbine rotation speeds. A smaller discretization of the distance has been carried out between positions 2 and 3, with a space step of 15 mm, i.e. 10 additional positions, for the flow velocity $U_\infty = 1.0$ m/s and for the design rotation speed ($TSR = 4$) only.

4 Acquisitions

The sampling frequency of the turbine parameters is $f_s = 128$ Hz for all the reference cases without the dummy tower. For every other case, the sampling frequency is $f_s = 256$ Hz. As explained in section 2.1, the sampling frequency is not constant for the 3C-LDV. Consequently, a time interpolation is required when processing a frequency analysis on these velocity data. The acquisition time is constant with 360 s for every run and the trigger is systematically used to synchronize both the acquisition systems (3C-LDV and turbine parameters). Three runs were recorded over a longer duration, i.e. 4200 s (`run067`, `run112` and `run167`, see table 12). These are associated with positions 2 and 3 of the dummy tower and without the dummy tower, and recorded for $U_\infty = 1.0$ m/s and $TSR = 4$ only.

The turbine acquisition files are located in the `LV/` folder and the 3C-LDV files are located in the `LDV/` folder. The turbine files are constituted of 18 rows including: the turbine rotation speed RPM, the thrust T, the torque Q and the 15 turbine load-cell components F_{xi}, F_{yi}, M_{xi}, M_{yi} and M_{zi} for blade $i = 1$ to 3. All the force and moment data are expressed in N or N m. The motor rotation speed is expressed in RPM. The 3C-LDV files are constituted of 10 rows: the number of the sample and 3 rows for every velocity component: the arrival time, the transit time and the velocity value. The arrival time, expressed in ms, corresponds to the time of the velocity value. The transit time, expressed in µs, corresponds to transit time of the particle inside the measurement volume. The velocity value is expressed in m/s and corresponds to every beam measurement LDAi, as explained in section 2.1.

Before every set of acquisition, a zero file is acquired to remove all the sensor offsets (excepted for the 3C-LDV). These files are named `zeroxxx.txt`. The corresponding zero is systematically removed from the following run files. There is no need to do it again during the post-processing.

Tables displayed on figures 9 to 12 resume all the acquired run files with their corresponding zeros and gives some details about the measurement conditions and the dummy tower position.

[1] For position 2, the turbine performance has not been measured for $U_\infty = 1.2$ m/s.

tank parameters			turbine rotation		distance		acquisition
ind.	vel.	turb.	TSR	RPM	tower – rotor		name
[-]	[m/s]	[%]	turbine	motor	[mm]		[-]
0	0.0	1.5	0.0	0		with no tower	zero001
662	0.8	1.5	0.0	0		with no tower	run001
662	0.8	1.5	1.0	549		with no tower	run002
662	0.8	1.5	2.0	1097		with no tower	run003
662	0.8	1.5	2.5	1372		with no tower	run004
662	0.8	1.5	3.0	1646		with no tower	run005
662	0.8	1.5	3.5	1920		with no tower	run006
662	0.8	1.5	4.0	2195		with no tower	run007
662	0.8	1.5	4.5	2469		with no tower	run008
662	0.8	1.5	5.0	2743		with no tower	run009
662	0.8	1.5	6.0	3292		with no tower	run010
662	0.8	1.5	7.0	3841		with no tower	run011
0	0.0	1.5	0.0	0		with no tower	zero002
827	1.0	1.5	0.0	0		with no tower	run012
827	1.0	1.5	1.0	686		with no tower	run013
827	1.0	1.5	2.0	1372		with no tower	run014
827	1.0	1.5	2.5	1715		with no tower	run015
827	1.0	1.5	3.0	2058		with no tower	run016
827	1.0	1.5	3.5	2401		with no tower	run017
827	1.0	1.5	4.0	2743		with no tower	run018
827	1.0	1.5	4.5	3086		with no tower	run019
827	1.0	1.5	5.0	3429		with no tower	run020
827	1.0	1.5	6.0	4115		with no tower	run021
827	1.0	1.5	7.0	4801		with no tower	run022
0	0.0	1.5	0.0	0		with no tower	zero003
992	1.2	1.5	0.0	0		with no tower	run023
992	1.2	1.5	1.0	823		with no tower	run024
992	1.2	1.5	2.0	1646		with no tower	run025
992	1.2	1.5	2.5	2058		with no tower	run026
992	1.2	1.5	3.0	2469		with no tower	run027
992	1.2	1.5	3.5	2881		with no tower	run028
992	1.2	1.5	4.0	3292		with no tower	run029
992	1.2	1.5	4.5	3704		with no tower	run030
992	1.2	1.5	5.0	4115		with no tower	run031
992	1.2	1.5	6.0	4938		with no tower	run032
992	1.2	1.5	7.0	5761		with no tower	run033
0	0.0	1.5	0.0	0	594	Position 0	zero004
662	0.8	1.5	0.0	0	594	Position 0	run034
662	0.8	1.5	1.0	549	594	Position 0	run035
662	0.8	1.5	2.0	1097	594	Position 0	run036
662	0.8	1.5	2.5	1372	594	Position 0	run037
662	0.8	1.5	3.0	1646	594	Position 0	run038
662	0.8	1.5	3.5	1920	594	Position 0	run039
662	0.8	1.5	4.0	2195	594	Position 0	run040
662	0.8	1.5	4.5	2469	594	Position 0	run041
662	0.8	1.5	5.0	2743	594	Position 0	run042
662	0.8	1.5	6.0	3292	594	Position 0	run043
662	0.8	1.5	7.0	3841	594	Position 0	run044

Figure 9 – Acquisitions carried out without the dummy tower and for position 0

tank parameters			turbine rotation		distance		acquisition
ind.	vel.	turb.	TSR	RPM	tower – rotor		name
[-]	[m/s]	[%]	turbine	motor	[mm]		[-]
0	0.0	1.5	0.0	0	594	Position 0	zero005
827	1.0	1.5	0.0	0	594	Position 0	run045
827	1.0	1.5	1.0	686	594	Position 0	run046
827	1.0	1.5	2.0	1372	594	Position 0	run047
827	1.0	1.5	2.5	1715	594	Position 0	run048
827	1.0	1.5	3.0	2058	594	Position 0	run049
827	1.0	1.5	3.5	2401	594	Position 0	run050
827	1.0	1.5	4.0	2743	594	Position 0	run051
827	1.0	1.5	4.5	3086	594	Position 0	run052
827	1.0	1.5	5.0	3429	594	Position 0	run053
827	1.0	1.5	6.0	4115	594	Position 0	run054
827	1.0	1.5	7.0	4801	594	Position 0	run055
0	0.0	1.5	0.0	0	594	Position 0	zero006
992	1.2	1.5	0.0	0	594	Position 0	run056
992	1.2	1.5	1.0	823	594	Position 0	run057
992	1.2	1.5	2.0	1646	594	Position 0	run058
992	1.2	1.5	2.5	2058	594	Position 0	run059
992	1.2	1.5	3.0	2469	594	Position 0	run060
992	1.2	1.5	3.5	2881	594	Position 0	run061
992	1.2	1.5	4.0	3292	594	Position 0	run062
992	1.2	1.5	4.5	3704	594	Position 0	run063
992	1.2	1.5	5.0	4115	594	Position 0	run064
992	1.2	1.5	6.0	4938	594	Position 0	run065
992	1.2	1.5	7.0	5761	594	Position 0	run066
0	0.0	1.5	0.0	0	427	Position 1	zero008
662	0.8	1.5	0.0	0	427	Position 1	run068
662	0.8	1.5	1.0	549	427	Position 1	run069
662	0.8	1.5	2.0	1097	427	Position 1	run070
662	0.8	1.5	2.5	1372	427	Position 1	run071
662	0.8	1.5	3.0	1646	427	Position 1	run072
662	0.8	1.5	3.5	1920	427	Position 1	run073
662	0.8	1.5	4.0	2195	427	Position 1	run074
662	0.8	1.5	4.5	2469	427	Position 1	run075
662	0.8	1.5	5.0	2743	427	Position 1	run076
662	0.8	1.5	6.0	3292	427	Position 1	run077
662	0.8	1.5	7.0	3841	427	Position 1	run078
0	0.0	1.5	0.0	0	427	Position 1	zero009
827	1.0	1.5	0.0	0	427	Position 1	run079
827	1.0	1.5	1.0	686	427	Position 1	run080
827	1.0	1.5	2.0	1372	427	Position 1	run081
827	1.0	1.5	2.5	1715	427	Position 1	run082
827	1.0	1.5	3.0	2058	427	Position 1	run083
827	1.0	1.5	3.5	2401	427	Position 1	run084
827	1.0	1.5	4.0	2743	427	Position 1	run085
827	1.0	1.5	4.5	3086	427	Position 1	run086
827	1.0	1.5	5.0	3429	427	Position 1	run087
827	1.0	1.5	6.0	4115	427	Position 1	run088
827	1.0	1.5	7.0	4801	427	Position 1	run089

Figure 10 – Acquisitions carried out for positions 0 & 1

tank parameters			turbine rotation		distance		acquisition
ind.	vel.	turb.	TSR	RPM	tower – rotor		name
[-]	[m/s]	[%]	turbine	motor	[mm]		[-]
0	0.0	1.5	0.0	0	427	Position 1	zero010
992	1.2	1.5	0.0	0	427	Position 1	run090
992	1.2	1.5	1.0	823	427	Position 1	run091
992	1.2	1.5	2.0	1646	427	Position 1	run092
992	1.2	1.5	2.5	2058	427	Position 1	run093
992	1.2	1.5	3.0	2469	427	Position 1	run094
992	1.2	1.5	3.5	2881	427	Position 1	run095
992	1.2	1.5	4.0	3292	427	Position 1	run096
992	1.2	1.5	4.5	3704	427	Position 1	run097
992	1.2	1.5	5.0	4115	427	Position 1	run098
992	1.2	1.5	6.0	4938	427	Position 1	run099
992	1.2	1.5	7.0	5761	427	Position 1	run100
0	0.0	1.5	0	0	260	Position 2	zero011
662	0.8	1.5	0.0	0	260	Position 2	run101
662	0.8	1.5	1.0	549	260	Position 2	run102
662	0.8	1.5	2.0	1097	260	Position 2	run103
662	0.8	1.5	2.5	1372	260	Position 2	run104
662	0.8	1.5	3.0	1646	260	Position 2	run105
662	0.8	1.5	3.5	1920	260	Position 2	run106
662	0.8	1.5	4.0	2195	260	Position 2	run107
662	0.8	1.5	4.5	2469	260	Position 2	run108
662	0.8	1.5	5.0	2743	260	Position 2	run109
662	0.8	1.5	6.0	3292	260	Position 2	run110
662	0.8	1.5	7.0	3841	260	Position 2	run111
0	0.0	1.5	0.0	0	260	Position 2	zero013
827	1.0	1.5	0.0	0	260	Position 2	run113
827	1.0	1.5	1.0	686	260	Position 2	run114
827	1.0	1.5	2.0	1372	260	Position 2	run115
827	1.0	1.5	2.5	1715	260	Position 2	run116
827	1.0	1.5	3.0	2058	260	Position 2	run117
827	1.0	1.5	3.5	2401	260	Position 2	run118
827	1.0	1.5	4.0	2743	260	Position 2	run119
827	1.0	1.5	4.5	3086	260	Position 2	run120
827	1.0	1.5	5.0	3429	260	Position 2	run121
827	1.0	1.5	6.0	4115	260	Position 2	run122
827	1.0	1.5	7.0	4801	260	Position 2	run123
0	0.0	1.5	0.0	0	93	Position 3	zero014
992	1.2	1.5	0.0	0	93	Position 3	run124
992	1.2	1.5	1.0	823	93	Position 3	run125
992	1.2	1.5	2.0	1646	93	Position 3	run126
992	1.2	1.5	2.5	2058	93	Position 3	run127
992	1.2	1.5	3.0	2469	93	Position 3	run128
992	1.2	1.5	3.5	2881	93	Position 3	run129
992	1.2	1.5	4.0	3292	93	Position 3	run130
992	1.2	1.5	4.5	3704	93	Position 3	run131
992	1.2	1.5	5.0	4115	93	Position 3	run132
992	1.2	1.5	6.0	4938	93	Position 3	run133
992	1.2	1.5	7.0	5761	93	Position 3	run134

Figure 11 – Acquisitions carried out for positions 1, 2 & 3

tank parameters			turbine rotation		distance		acquisition
ind. [-]	vel. [m/s]	turb. [%]	TSR turbine	RPM motor	tower – rotor [mm]		name [-]
0	0.0	1.5	0.0	0	93	Position 3	zero015
827	1.0	1.5	0.0	0	93	Position 3	run135
827	1.0	1.5	1.0	686	93	Position 3	run136
827	1.0	1.5	2.0	1372	93	Position 3	run137
827	1.0	1.5	2.5	1715	93	Position 3	run138
827	1.0	1.5	3.0	2058	93	Position 3	run139
827	1.0	1.5	3.5	2401	93	Position 3	run140
827	1.0	1.5	4.0	2743	93	Position 3	run141
827	1.0	1.5	4.5	3086	93	Position 3	run142
827	1.0	1.5	5.0	3429	93	Position 3	run143
827	1.0	1.5	6.0	4115	93	Position 3	run144
827	1.0	1.5	7.0	4801	93	Position 3	run145
0	0.0	1.5	0.0	0	93	Position 3	zero016
662	0.8	1.5	0.0	0	93	Position 3	run156
662	0.8	1.5	1.0	549	93	Position 3	run157
662	0.8	1.5	2.0	1097	93	Position 3	run158
662	0.8	1.5	2.5	1372	93	Position 3	run159
662	0.8	1.5	3.0	1646	93	Position 3	run160
662	0.8	1.5	3.5	1920	93	Position 3	run161
662	0.8	1.5	4.0	2195	93	Position 3	run162
662	0.8	1.5	4.5	2469	93	Position 3	run163
662	0.8	1.5	5.0	2743	93	Position 3	run164
662	0.8	1.5	6.0	3292	93	Position 3	run165
662	0.8	1.5	7.0	3841	93	Position 3	run166
827	1.0	1.5	4.00	2743	**108**		run146
827	1.0	1.5	4.00	2743	**123**		run147
827	1.0	1.5	4.00	2743	**138**		run148
827	1.0	1.5	4.00	2743	**153**		run149
827	1.0	1.5	4.00	2743	**168**		run150
827	1.0	1.5	4.00	2743	**183**		run151
827	1.0	1.5	4.00	2743	**198**		run152
827	1.0	1.5	4.00	2743	**213**		run153
827	1.0	1.5	4.00	2743	**228**		run154
827	1.0	1.5	4.00	2743	**243**		run155
827	1.0	1.5	4.0	2743	93	Position 3	run067
827	1.0	1.5	4.0	2743	260	Position 2	run112
827	1.0	1.5	4.0	2743		with no tower	run167

Figure 12 – Acquisitions carried out for position 3 and for every additional positions between positions 2 & 3. The three runs recorded over the long duration (4200 s) are at the very end of this table as well.

References

Dantec Dynamics (2018). *Measurement Principles of LDA*. URL: https://www.dantecdynamics.com/solutions-applications/solutions/fluid-mechanics/laser-doppler-anemometry-lda/measurement-principles-of-lda/ (visited on 05/15/2018).

Deskos, G., G. S. Payne, B. Gaurier, and M. Graham (2020). "On the spectral behaviour of the turbulence-driven power fluctuations of horizontal-axis turbines". In: *Journal of Fluid Mechanics* 904, A13. DOI: 10.1017/jfm.2020.681.

Gaurier, B., G. Germain, and J.-V. Facq (2017). "Experimental study of the Marine Current Turbine behaviour submitted to macro-particle impacts". In: *12th European Wave and Tidal Energy Conference*. Cork, Ireland. URL: https://ewtec.org/proceedings/.

Gaurier, B., G. Germain, J.-V. Facq, and T. Bacchetti (2018). *Wave and current flume tank of IFREMER at Boulogne-sur-mer. Description of the facility and its equipment*. en. Tech. rep. Ifremer. DOI: 10.13155/58163.

Gaurier, B., G. Germain, J.-V. Facq, C. Johnstone, A. D. Grant, A. H. Day, E. Nixon, F. Di Felice, and M. Costanzo (2015). "Tidal energy "round Robin" tests comparisons between towing tank and circulating tank results". In: *International Journal of Marine Energy* 12, pp. 87–109. DOI: 10.1016/j.ijome.2015.05.005.

Gaurier, B., M. Ikhennicheu, G. Germain, and P. Druault (2020a). "Experimental study of bathymetry generated turbulence on tidal turbine behaviour". In: *Renewable Energy* 156, pp. 1158–1170. DOI: 10.1016/j.renene.2020.04.102.

Gaurier, B., S. Ordonez-Sanchez, J.-v. Facq, G. Germain, C. Johnstone, R. Martinez, F. Salvatore, I. Santic, T. Davey, C. Old, and B. Sellar (2020b). "MaRINET2 Tidal Energy Round Robin Tests-Performance Comparison of a Horizontal Axis Turbine Subjected to Combined Wave and Current Conditions". In: *Journal of Marine Science and Engineering* 8.6, p. 463. DOI: 10.3390/jmse8060463.

Mason-Jones, A., D. M. O'Doherty, C. E. Morris, and T. O'Doherty (2013). "Influence of a velocity profile & support structure on tidal stream turbine performance". In: *Renewable Energy* 52, pp. 23–30. DOI: 10.1016/j.renene.2012.10.022.

Payne, G. S., T. Stallard, R. Martinez, and T. Bruce (2018). "Variation of loads on a three-bladed horizontal axis tidal turbine with frequency and blade position". In: *Journal of Fluids and Structures* 83.2018, pp. 156–170. DOI: 10.1016/j.jfluidstructs.2018.08.010.

Symétrie technology (2020). *MISTRAL - Hexapods of movement*. URL: https://symetrie.fr/en/hexapods/mistral/ (visited on 09/06/2021).